MEDICAL ACUPUNCTURE
Volume 31, Number 3, 2019

DOI: 10.1089/acu.2019.1334

Innervated Properties of Acupuncture Points LI 4 and LR 3 in the Rat: Neural Pathway Tracing with Cholera Toxin Subunit B

Jingjing Cui, MD, PhD, Jia Wang, MD, PhD, and Wanzhu Bai, MD, PhD

ABSTRACT

Objective: Increasing evidence from acupuncture research suggests that the nervous system corresponds closely with classical acupuncture points. The aim of this research was to provide neuroanatomical evidence for revealing the innervated properties of different acupuncture points through comparing the sensory and motor pathways associated with *Hegu* (LI 4) and *Taichong* (LR 3) in rat extremities.

Materials and Methods: Cholera toxin subunit B (CTB) was injected into LI 4 and LR 3 in different rats, and CTB neural labeling was examined using fluorescent immunohistochemistry and observed under fluorescent microscopy in the corresponding areas from the peripheral nervous system to the central nervous system, including the dorsal root ganglia (DRG), spinal cord, and brainstem.

Results: When LI 4 was injected with CTB, CTB-labeled sensory neurons ranged from C–5 to T–1 DRG, and their transganglionic axons terminated in the C–5 to C–8 spinal dorsal horn as far as the cuneate nucleus, while labeled motor neurons were located in the C–7 to T–1 spinal ventral horn. In contrast, similar neural labeling was observed for LR 3 CTB injection, with an orderly arrangement in the L–3 to L–5 DRG, L–3 to L–5 spinal dorsal horn, gracile nucleus, and L–4 to L–6 spinal ventral horn.

Conclusions: The present results provide further evidence to aid understanding of the differential innervation of acupuncture points LI 4 and LR 3. This innervation establishes its connection with the nervous system in a distinct segmental and regional pattern through the spinal sensory and motor pathways.

Keywords: acupuncture point, neural tracing, innervation, cholera toxin subunit B, sensory neurons, motor neurons

INTRODUCTION

Most understanding of the acupuncture points is based on the traditional meridian theory and the points' anatomical locations.[1,2] Increasing evidence from neuroanatomical and neuroembryologic research has shown that classical acupuncture points are closely correlated with the nervous system.[3–6] However, the innervation of the acupuncture points was mainly introduced from the perspective of the peripheral nervous system (PNS); how these nerves originated from and terminated in the central nervous system (CNS) was mentioned less. In order to observe the detailed innervation of acupuncture points in the extremities, *Hegu* (LI 4) and *Taichong* (LR 3) were selected as representative points in the rat and traced with cholera toxin subunit B (CTB). As a retrograde and transganglionic tracer, CTB was used to label the sensory neurons, transganglionic axons, and motor neurons from the PNS to the CNS.[7,8] This advantage of CTB was applied to demonstrate sensory and motor innervation of the two acupuncture points.[9–11] With this neural-tracing technique, the current authors expected to determine the innervated properties of LI 4 and LR 3, and examine their differences from the spinal sensory and motor pathways. This research could provide valuable insight for understanding the neuroanatomical characteristics of other acupuncture points in the extremities.

Institute of Acupuncture and Moxibustion, China Academy of Chinese Medical Sciences, Beijing, China.

MATERIALS AND METHODS

Experimental Animals

Six young-adult, male Sprague–Dawley rats (8–10 weeks old, weighing 225 ± 25 g) were used in this study. The animals were provided by the Institute of Laboratory Animal Sciences, of the Chinese Academy of Medical Sciences. The license number was SCKX (JUN) 2016-004. All animals were subjected to a 12-hour light/dark cycle with controlled temperature and humidity and allowed free access to food and water. All animal experiments were approved by the the ethics committee of the Institute of Acupuncture and Moxibustion, China Academy of Chinese Medical Sciences, Beijing, China (reference no. 20160011), and carried out in accordance with the regulations provided by the U.S. *National Institutes of Health Guide for the Care and Use of Laboratory Animals*.[12]

Microinjection of CTB

Microinjection was carried out on the LI 4 ($n = 3$) and LR 3 ($n = 3$) points, which belong to the Large Intestine and Liver meridians, respectively. The corresponding sites of LI 4 and LR 3 in the rat were determined according to the principle of comparative anatomy, in which LI 4 is located on the dorsum of the forefoot, radial to the midpoint of the second metacarpal bone, and LR 3 is located on the dorsum of the hind foot, between the first and second metatarsal bones (Fig. 1). Under anesthesia with isoflurane, a total of 4 μL of 1% CTB (List Biological Labs, Campbell, CA) solution was injected slowly into LI 4 or LR 3 on the left side. The depth of the injection was $\sim$2–3 mm.

Perfusion

On the third surviving day, the rats were anesthetized deeply with ether (Beijing Chemical Plant, Beijing, China) and transcardially perfused with 100 mL of 0.9% saline immediately followed by 300 mL of 4% paraformaldehyde in 0.1 M of phosphate buffered solution (PB, pH 7.4). The brainstem, spinal cord, and associated dorsal root ganglia (DRG) were dissected out and stored in 30% sucrose PB at 4°C.

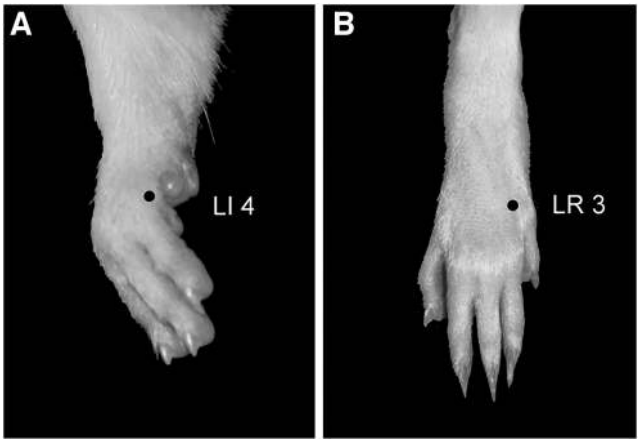

FIG. 1. LI 4 **(A)** and LR 3 **(B)** in rat forefoot and hind foot respectively (dot).

Sections

Serial transverse sections of the brainstem and spinal cord, and sagittal sections of the DRG were cut at a thickness of 40 μm on a freezing microtome (Microm International HM 430, Thermo, Germany). All sections were collected in an orderly fashion, placed in a 6-hole Petri dish, and floated in 0.1 M of PB (pH 7.4).

Fluorescent Immunohistochemistry

One in every sixth sections of the brainstem and spinal cord, and all sections of the DRG were prepared for fluorescent immunohistochemistry. Sections were incubated in a blocking solution containing 3% of normal rabbit serum and 0.5% of Triton X-100 in 0.1 M of PB for 1 hour, then transferred to goat anti-CTB (List Biological Labs, Campbell, CA) at a dilution of 1:1000 in 0.1 M of PB containing 1% rabbit serum and 0.5% Triton X-100 for overnight storage at 4°C. On the following day, after washing three times with 0.1 M of PB, the sections were exposed to rabbit anti-goat Alexa Fluor 488 secondary antibody (1:500; Molecular Probes, Eugene, OR) for 2 hours and then washed with 0.1 M of PB. After that, the sections were mounted on gelatin-coated glass slides. Finally, the slides were coverslipped with 50% glycerin before observation.

Observation

The anatomical structures of the tissue sections from the brainstem and spinal cord were determined cytoarchitecturally based on *The Rat Brain in Stereotaxic Coordinates*,[13] and segments of DRG were counted as the locations of the vertebra. All tissue samples were viewed and the observations were recorded with a fluorescent microscope (Y-IDP, Nikon Co., Tokyo, Japan) equipped with a digital camera (DMX1200C, Nikon, Japan). All images were processed using Adobe PhotoShop CS5 and Adobe Illustrator CS5 (Adobe Systems, San Jose, CA), in which only brightness and contrast were adjusted.

Statistical Analysis

Data were expressed as mean ± standard deviation, and processed with statistical software from SPSS 16.0.

RESULTS

Under the fluorescence microscope, CTB labeling appeared green, and all neural labeling was located ipsilaterally

on the injection side, including the sensory neurons (Fig. 2), transganglionic axons (Fig. 3), and motor neurons (Fig. 4).

Sensory Neurons

The CTB-labeled sensory neurons were noted in DRG (Fig. 2). Where LI 4 injection was performed, labeled sensory neurons ranged from cervical (C–5) to thoracic (T–1) DRG. The number of CTB-labeled sensory neurons was counted in 10 sections from each DRG. A total of 518 labeled sensory neurons was counted from C–5 to T–1 DRG, which were arranged in a fairly orderly fashion within C–7: 64 ± 13.9>C–6: 51.7 ± 10.4>C–8: 35.7 ± 4.5>T–1: 13 ± 6.5>C–5: 8.3 ± 1.5 ($n = 3$). In contrast, where LR 3 injection was performed, 702 labeled sensory neurons were counted in lumbar (L–3 to L–5) DRG, and sequentially distributed in L–4: 142.7 ± 41.1>L3: 75.7 ± 15.3>L5: 15.6 ± 3.8 ($n = 3$).

Transganglionic Axons

Following the labeled sensory neurons in DRG, their transganglionic axons were noted in the spinal dorsal horn and brainstem (Fig. 3).

The transganglionic axons associated with LI 4 were found to be dense in the medial part of the spinal dorsal horn from the C–5 to C–8 segments as far as in the cuneate nucleus (Fig. 3A, B, A1, and B1). Comparatively, where LR 3 injection was performed, the transganglionic axons terminated in the medial part from the L–3 to the L–5 spinal dorsal horn, and in the gracile nucleus (Fig. 3C, D, C1, and D1).

Motor Neurons

In both cases, the labeled motor neurons were mainly located at the dorsolateral part of the spinal ventral horn (Fig. 4). Where LI 4 was injected, labeled motor neurons were detected from the C–7 to the T–1 segments with a high concentration at C–8 (Fig. 4A and A1). As a comparison, the labeled motor neurons associated with LR 3 were located from the L–4 to the L–6 segments and concentrated at the L–5 segment (Fig. 4B and B1). In this study, there were 86 and 160 labeled motor neurons counted from 30 representative spinal transverse sections for LI 4 and LR 3, respectively. Because there are no distinct boundaries between spinal segments, the number of labeled motor neurons was not distinguished further at each spinal segment.

DISCUSSION

The present study showed the neuroanatomical characteristics of acupuncture points LI 4 and LR 3 in the rat, using a neural-tract tracing technique, providing an outline for understanding innervation of acupuncture points at the extremities via the distinct spinal sensory and motor pathways (Fig. 5).

As is known, there are two different perspectives on the selection of acupuncture points to address clinical situations. One consideration is based on traditional meridian theory, and the other consideration is based on current knowledge of anatomy, physiology, and pathology.[3,14–16] Obviously, the present observations were focused on the latter, especially on the neuroanatomical characteristics of acupuncture points from the PNS to the CNS.

From the perspective of the PNS, it is well-known that acupuncture points on the trunk, arms, and legs accept segmental innervations that are classified according to their myotomes or dermatomes[3–5]; however, how these peripheral nerves are connected to the CNS is less well-known. The present study provides further neuroanatomical evidence from the CNS to show the different sensory and motor innervations of acupuncture points in the rat forelimb and hind limb.

Considering the distribution of neural labeling in the DRG, spinal dorsal and ventral horns, and cuneate or gracile nucleus, it was clear that LI 4 and LR 3 had established their own neural connections with their corresponding targets in segment- and region-specific patterns from the PNS to the CNS. The same innervated pattern was also seen in previous studies on PC 8 and KI 1.[9,10]

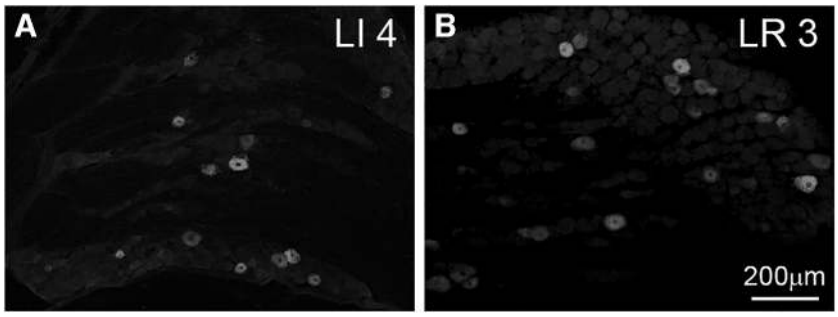

FIG. 2. Representative photographs of the cholera toxin subunit B–labeled sensory neurons in dorsal root ganglia associated with LI 4 **(A)** and LR 3 **(B)**. Same scale bar for **A** and **B**.

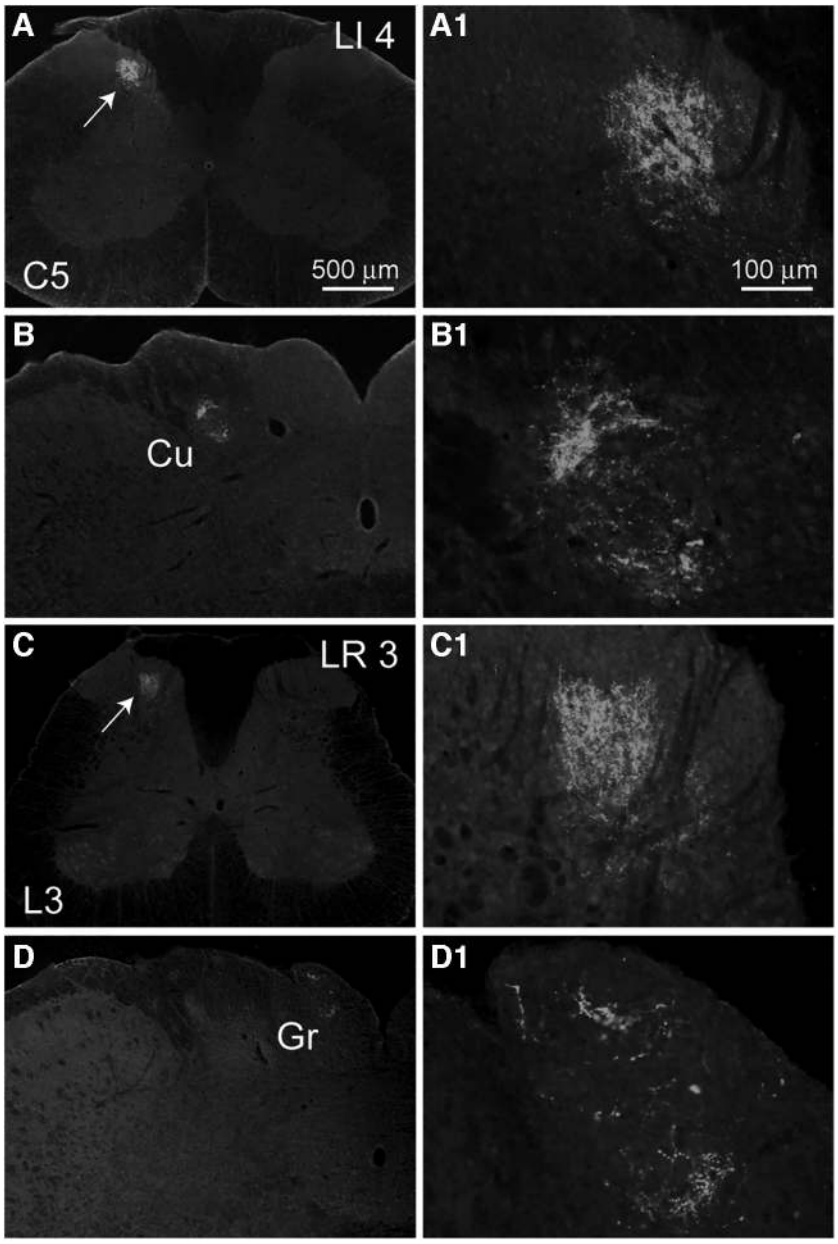

FIG. 3. Distribution of the cholera toxin subunit B–labeled transganglionic axons in the spinal dorsal horn and brainstem. (**A–D**) Representative photographs of the labeled axon terminals in the cervical (C–5) spinal cord (**A,** *arrow*) and the cuneate nucleus (Cu, **B**) for LI 4, as well as in the lumbar (L–3) spinal cord (*C, arrow*), and the gracile nucleus (Gr, **D**) for LR 3. Same scale bar in **A–D**. (**A1–D1**) Magnified photos from **A–D** showing the labeled axon terminals in detail. Same scale bar in **A1–D1**.

By comparing the distribution of neural labeling associated with these acupuncture points, it can be concluded that the spinal cervical enlargement and cuneate nucleus are mainly correlated with innervations on acupuncture points from the forelimb, and that the spinal lumbar enlargement and gracile nucleus are closely correlated with acupuncture points from the hind limb. Interestingly, on the one hand, sensory afferents from the acupuncture points at the distal parts of the forelimb or hind limb to the spinal cord are distributed in similar patterns—both terminate in the medial part of the spinal dorsal horn. On the other hand, the motor efferents to these points originate from the neurons at the dorsolateral part of the spinal ventral horn. These region-specific connections between different acupuncture points and the nervous system are obviously arranged in a somatotopic organization. This somatotopic organization has been presented well in previous neural-tracing studies, including the sensory afferent terminals from different peripheral areas

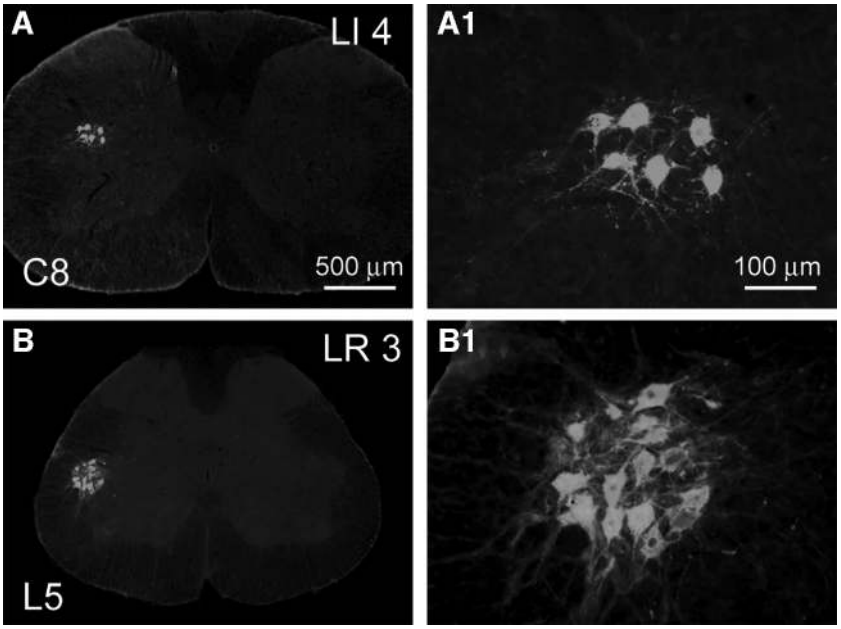

FIG. 4. Distribution of the cholera toxin subunit B–labeled motor neurons in the spinal cord. **(A and B)** Representative photographs of the labeled motor neurons in the cervical (C–8) spinal cord for LI 4 **(A)**, and in the lumbar (L–5) spinal cord for LR 3 **(B)**. Same scale bar in **A** and **B**. **(A1 and B1)** Magnified photographs from **A** and **B** showing the labeled motor neurons in detail. Same scale bar in **A1** and **B1**.

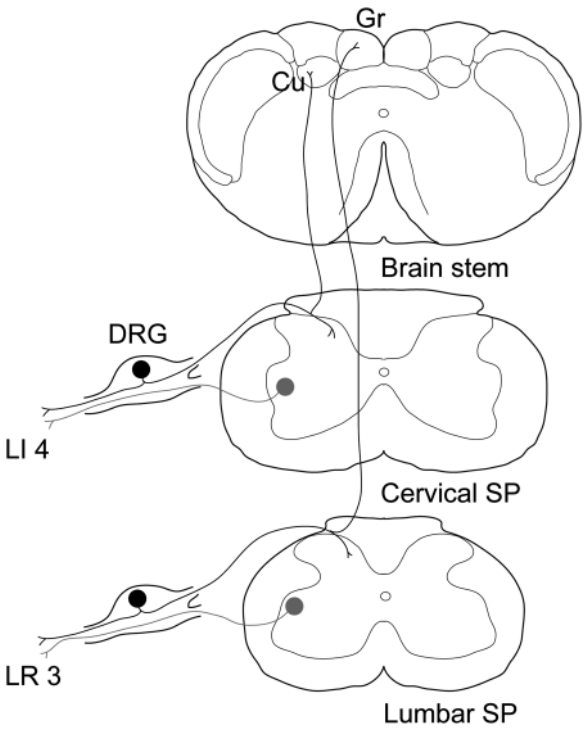

FIG. 5. The sensory and motor pathways from the acupuncture points to the nervous system. Acupuncture points LI 4 and LR 3 establish their own neural connections with their corresponding targets in the dorsal root ganglion (DRG), spinal dorsal and ventral horns, and cuneate nucleus (Cu) or gracile nucleus (Gr), via spinal sensory (black) and motor (gray) pathways. SP, spinal cord.

to the spinal dorsal horn and brainstem, as well as motor efferents from the spinal ventral horn.[17–21]

As a comparison, innervation on acupuncture points located on the head and face is more complicated.[6,11] For example, GB 14, ST 2, and ST 6 establish their sensory connections with the trigeminal ganglion, cervical DRG, spinal trigeminal nucleus, and cervical spinal dorsal horn via trigeminal and spinal sensory pathways, as well as making motor connections with the facial nucleus, motor trigeminal nucleus, and cervical spinal ventral horn via trigeminal, facial and spinal motor pathways.[11] These analyses not only clarify the innervated properties of acupuncture points from the PNS but also reveal the specific connections between acupuncture points and their corresponding regions in the CNS. This kind of structural connection is helpful for determining the differential innervations between the different acupuncture points from the spinal sensory and motor pathways, which might be responsible for transmission of acupuncture signals from the acupuncture points to the nervous system. Therefore, this knowledge can guide the choice of proper acupuncture points to meet the experimental and clinical demands.

Although the present study revealed the accurate positions of neural labeling associated with LI 4 and LR 3 in the rat nervous system, due to the technical limitations of CTB itself, labeling in the DRG, spinal dorsal and ventral horns, and cuneate or gracile nucleus belongs to the first-order neural elements along the multiorder neural pathways from the PNS

to the CNS.[17–21] Their successive neural connections with the corresponding targets in the spinal cord, thalamus, and cerebral cortex was not determined in the current study. In 2016 and 2018, results from functional magnetic resonance imaging (fMRI) studies indicated that acupuncture stimulation at LR 3 can specifically activate or deactivate the visual, motor, and sensory cortices, etc., while stimulating both LI 4 and LR 3 can modulate activities of cognition-related brain regions in patients with Alzheimer's disease.[22,23] These second or higher-order neuroanatomical connections from the acupuncture points to the nervous system might be observed by using a transsynaptic-tracing technique with a neurotropic virus.[24,25]

CONCLUSIONS

The sensory and motor connections from LI 4 and LR 3 to their corresponding targets in the nervous system were shown by using a CTB neural-tracing technique. Considering the multiorder neural pathways from the PNS to the CNS, this tracing is only the first step toward understanding the innervated properties of the acupuncture points in the extremities via spinal sensory and motor pathways; the next- and higher-order neural connections of these points to the CNS remain to be elucidated.

ACKNOWLEGMENTS

This study was funded by the National Natural Science Foundation of China (Project Code No. 81774211; No. 81774432).

AUTHOR DISCLOSURE STATEMENT

No competing financial interests exist.

REFERENCES

1. Liang FR. *Acupuncturology.* Beijing: China Press of Traditional Chinese Medicine; 2005:47&134.
2. Huang LX. *WHO Standard Acupuncture Point Locations in the Western Pacific Region.* Beijing: People's Medical Publishing House; 2010:34&190.
3. Cheng KJ. Neuroanatomical characteristics of acupuncture points: Relationship between their anatomical locations and traditional clinical indications. *Acupunct Med.* 2011;29(4): 289–294.
4. Dorsher PT. Neuroembryology of the acupuncture principal meridians: Part1. The extremities. *Med Acupunct*. 2017;29(1): 10–19.
5. Dorsher PT. Neuroembryology of the acupuncture principal meridians: Part 2. The trunk. *Med Acupunct*. 2017;29(2): 77–86.
6. Dorsher PT, Chiang P. Neuroembryology of the acupuncture principal meridians: Part 3. The Head and Neck. *Med Acupunct*. 2018;30(2):80–86.
7. Hirakawa M, McCabe JT, Kawata M. Time-related changes in the labeling pattern of motor and sensory neurons innervating the gastrocnemius muscle, as revealed by the retrograde transport of the cholera toxin B subunit. *Cell Tissue Res.* 1992;267(3):419–427.
8. Rivero-Melian C, Rosario C, Grant G. Demonstration of transganglionically transported choleragenoid in rat spinal cord by immunofluorescence cytochemistry. *Neurosci Lett.* 1992;145(1):114–117.
9. Cui JJ, Ha LJ, Zhu XL, Shi H, Wang FC, Jing XH, Bai WZ. Neuroanatomical basis for acupuncture point PC8 in the rat: Neural tracing study with cholera toxin subunit B. *Acupunct Med.* 2013;31(4):389–394.
10. Ha LJ, Cui JJ, Zhu XL, Wang FC, Jing XH, Bai WZ. Segmental and regional distribution of neurons and their axonal projection associated with acupoint ''*yongquan*'' (KI 1) in the rat: Cholera toxin subunit B method [in Chinese]. *Zhen Ci Yan Jiu.* 2013;38(5):375–379.
11. Wang J, Cui J, She C, Xu D, Zhang Z, Wang H, Bai W. Differential innervation of tissues located at traditional acupuncture points in the rat forehead and face. *Acupunct Med.* 2018;36(6):408–414.
12. National Institutes of Health. *National Institutes of Health Guide for the Care and Use of Laboratory Animals.* Washington, DC: National Academy Press; 1996.
13. Paxinos G, Watson C. *The Rat Brain in Stereotaxic Coordinates.* San Diego: Academic Press; 1998:figs.70–78;117a; &117b.
14. Karavis M. The neurophysiology of acupuncture: A viewpoint. *Acupunct Med.* 1997;15(1):33–42.
15. Zhao ZQ. Neural mechanism underlying acupuncture analgesia. *Prog Neurobiol.* 2008;85(4):355–375.
16. White A. Western medical acupuncture: A definition. *Acupunct Med.* 2009;27(1):33–35.
17. Maslany S, Crockett DP, Egger MD. Somatotopic organization of the dorsal column nuclei in the rat: Transganglionic labeling with B-HRP and WGA-HRP. *Brain Res.* 1991; 564(1):56–65.
18. Maslany S, Crockett DP, Egger MD. Organization of cutaneous primary afferent fibers projecting to the dorsal horn in the rat: WGA-HRP versus B-HRP. *Brain Res.* 1992;569(1):123–135.
19. Panneton WM, Gan Q, Juric R. The central termination of sensory fibers from nerves to the gastrocnemius muscle of the rat. *Neuroscience.* 2005;134(1):175–187.
20. Odagaki K, Kameda H, Hayashi T, Sakurai M. Mediolateral and dorsoventral projection patterns of cutaneous afferents within transverse planes of the mouse spinal dorsal horn. *J Comp Neurol.* 2019;527(5):972–984.
21. Takahashi Y, Ohtori S, Takahashi K. Somatotopic organization of lumbar muscle–innervating neurons in the ventral horn of the rat spinal cord. *J Anat.* 2010;216(4): 489–495.

22. Zheng Y, Wang Y, Lan Y, et al. Imaging of brain function based on the analysis of functional connectivity–imaging analysis of brain function by fMRI after acupuncture at LR3 in healthy individuals. *Afr J Tradit Complement Altern Med.* 2016;13(6):90–100.
23. Zheng W, Su Z, Liu X, et al. Modulation of functional activity and connectivity by acupuncture in patients with Alzheimer disease as measured by resting-state fMRI. *PLoS One.* 2018; 13(5):e0196933.
24. Dum RP, Strick PL. Transneuronal tracing with neurotropic viruses reveals network macroarchitecture. *Curr Opin Neurobiol.* 2013;23(2):245–249.
25. Zingg B, Chou XL, Zhang ZG, Mesik L, Liang F, Tao HW, Zhang LI. AAV-mediated anterograde transsynaptic tagging: Mapping corticocollicular input–defined neural pathways for defense behaviors. *Neuron*. 2017;93(1):33–47.

Address correspondence to:
Wanzhu Bai, MD, PhD
Institute of Acupuncture and Moxibustion
China Academy of Chinese Medical Sciences
No. 16 Nanxiaojie of Dongzhimen
Dongcheng District
Beijing 100700
China

E-mail: wanzhubaisy@hotmail.com